Available online at www.sciencedirect.com
ScienceDirect
Journal of Solid State Chemistry 179 (2006) 3599–3606
JOURNAL OF SOLID STATE CHEMISTRY
www.elsevier.com/locate/jssc

In situ X-ray powder diffraction, synthesis, and magnetic properties of $InVO_3$

Rylan J. Lundgren[a], Lachlan M.D. Cranswick[b], Mario Bieringer[a,*]

[a]*Department of Chemistry, University of Manitoba, Winnipeg, MB, Canada R3T 2N2*
[b]*Canadian Neutron Beam Centre, National Research Council Canada, Chalk River Laboratories, Chalk River, Ont., Canada K0J 1J0*

Received 3 June 2006; received in revised form 13 July 2006; accepted 14 July 2006
Available online 29 July 2006

Abstract

We report the first synthesis and high-temperature in situ X-ray diffraction study of $InVO_3$. Polycrystalline $InVO_3$ has been prepared via reduction of $InVO_4$ using a carbon monoxide/carbon dioxide buffer gas. $InVO_3$ crystallizes in the bixbyite structure in space group *Ia–3* (206) with $a = 9.80636(31)$ Å with In^{3+}/V^{3+} disorder on the (8*b*) and (24*d*) cation sites. In situ powder X-ray diffraction experiments and thermal gravimetric analysis in a CO/CO_2 buffer gas revealed the existence of the metastable phase $InVO_3$. Bulk samples with 98.5(2)% purity were prepared using low-temperature reduction methods. The preparative methods limited the crystallinity of this new phase to approximately 225(50) Å. Magnetic susceptibility and neutron diffraction experiments suggest a spin-glass ground state for $InVO_3$.
© 2006 Elsevier Inc. All rights reserved.

Keywords: $InVO_3$; V(III); In situ powder X-ray diffraction; Crystal structure; Bixbyite; Magnetism; Powder neutron diffraction

1. Introduction

The AVO_3 series with A = rare earth has been extensively investigated because of interesting magnetic and structural properties such as canted antiferromagnetic ground states coupled with orbital ordering [1] and low-temperature magnetic field-dependent spin reversal [2].

AVO_3 (A = Ln, Y) compounds form distorted orthorhombic perovskite structures isostructural with $GdFeO_3$ [3,4]. With decreasing A^{3+} cation radii the VO_6 octahedra undergo cooperative tilting resulting in decreased V–O–V bond angles from 157.8° and 156.7° in $LaVO_3$ to 144.8° and 144.3° in YVO_3 [5–8]. Lu^{3+} is the smallest known A^{3+} cation forming a stable AVO_3 perovskite structure. Sc^{3+} is too small to stabilize the perovskite structure, instead a cubic bixbyite structure with Sc/V disorder on the two available crystallographic cation sites is found [9,10]. Recently, the AVO_3 perovskites have been investigated for their magnetic properties. At low temperatures the formation of canted antiferromagnetic structures has been reported. The Neel temperatures (T_N) monotonically decrease with decreasing A^{3+} cation sizes, with T_N ranging from 156 to 135 K for $LaVO_3$ to 101 K for $LuVO_3$ [11,12]. The AVO_3 systems have shown very interesting magnetic behavior and have been the focus of many structure–property studies since it was reported that $LaVO_3$ cannot be conveniently described as a spin only system as the cubic crystalline field does not completely quench the orbital angular momentum [13]. Furthermore, multiple and reversible sign changes in magnetism with changing temperature and magnetic fields have been observed for $LaVO_3$, $CeVO_3$, and YVO_3 [14,15]. These effects are seen to be the result of a first-order magnetorestrictive distortion at a temperature below that of the magnetic ordering. For A = La, Ce, Y, Yb, and Lu additional crystallographic phase transitions from orthorhombic to monoclinic have been reported below the magnetic ordering temperature [6–9]. The structure and magnetism of the AVO_3 series have made them the subject of numerous studies concerning the interplay between orbital ordering and lattice distortion over a range of temperatures [15] and interest in these phases appears to only increase as further studies are conducted to explore their intriguing physical properties.

*Corresponding author. Fax: +1 204 474 7608.
E-mail address: Mario_Bieringer@umanitoba.ca (M. Bieringer).

0022-4596/$ - see front matter © 2006 Elsevier Inc. All rights reserved.
doi:10.1016/j.jssc.2006.07.037

Notably, most work has been carried out on AVO_3 where A is diamagnetic, i.e. A = La, Lu and Y.

In contrast to the perovskites very little is known about the bixbyite phase $ScVO_3$ [9,10]. The cubic crystal structure and the magnetization between 77 and 300 K [9] have been reported, but no details about low-temperature magnetism have been published. Even more surprising $InVO_3$ has never been reported. The ionic radius of In^{3+} is in between Sc^{3+} and Lu^{3+}. This raises the question regarding the crystallographic structure of $InVO_3$. It is noteworthy that $InVO_3$ was predicted to crystallize in space $P6_3/mmc$ [16]. Furthermore $InVO_3$ only contains one paramagnetic ion, $V^{3+} = d^2$, and is therefore a good model compound for the investigation of V^{3+} magnetism.

The synthesis of the known polycrystalline AVO_3 phases is straight forward facilitating the direct reaction of A_2O_3 and V_2O_3 at temperatures between 1000 and 1500 °C in argon or alternatively the reduction of AVO_4 in hydrogen at about 1000 °C.

We are reporting for the first time the synthesis of the missing member $InVO_3$. Our report provides insights into the stability of this new phase and presents first data regarding the magnetic properties of $InVO_3$. $InVO_3$ cannot be prepared by high-temperature techniques primarily due to the similar redox potentials for $In \rightarrow In^{3+}$ and $V^{3+} \rightarrow V^{5+}$. In fact the reduction potentials in aqueous solution favor the reduction of In^{3+} to In^0 over V^{5+} to V^{3+} reduction. The high-temperature reduction of $InVO_4$ results in indium metal formation whereas the direct solid state reaction of the sesquioxides in an inert atmosphere does not undergo any reaction at all. Our powder X-ray in situ diffraction studies have provided us with the appropriate conditions for the bulk synthesis of $InVO_3$.

3. Experimental

3.1. Synthesis

3.1.1. In situ powder X-ray diffraction

In situ powder X-ray diffraction experiments were carried out on a PANalytical X'Pert Pro diffractometer equipped with an X'Celerator detector and an Anton Paar HTK2000 high-temperature camera. Using Cu$K\alpha_{1,2}$ (λ = 1.540598, 1.544426 Å) radiation diffraction data were obtained for the angular range 2θ = 15–65° using 0.0167° steps. The $InVO_4$ sample was mounted as a thin layer on a platinum heating element. The sample was heated in a 1:3 CO/CO_2 gas flow and 30 min. Diffractograms were measured from 25 to 1000 °C at 25 °C increments. The temperature of the furnace is accurate within at least 5 °C between room temperature and 1200 °C.

3.1.2. Preparation of bulk samples

Polycrystalline $InVO_3$ was prepared via solid state synthesis of $InVO_4$ followed by reduction in a CO/CO_2 buffer gas:

(a) $InVO_4$ was prepared by solid state reaction from In_2O_3 (Alfa Aesar 99.995%) and NH_4VO_3 (Cerac 99.9%) according to Eq. (1):

$$In_2O_3 + 2NH_4VO_3 \rightarrow 2InVO_4 + 2NH_3 + H_2O \quad (1)$$

NH_4VO_3 was supplied in slight excess (2 mol%) in order to compensate for vanadium oxide loss during the synthesis. The starting materials were ground in an agate mortar and heated in oxygen at 1000 °C for 12 h with one intermediate grinding. The resulting highly

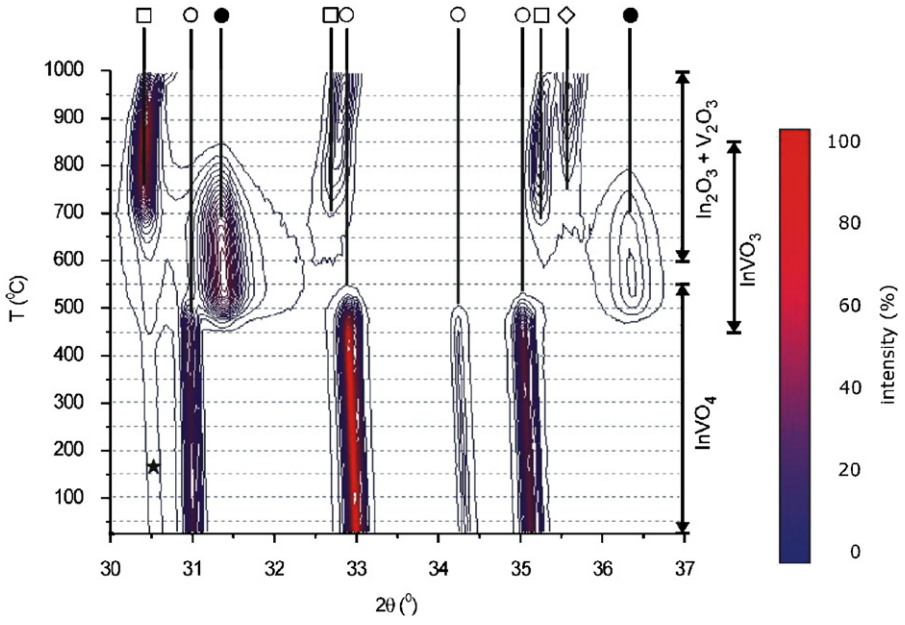

Fig. 1. Contour plot of powder X-ray diffractograms from 25 to 1000 °C using 25 °C increments. The intensity scale is indicated on the right. All contour levels are plotted using constant increments. Diffraction peaks are labeled as follows: $InVO_4$ = open circles, $InVO_3$ = solid circles, In_2O_3 = open squares and V_2O_3 = open diamonds. The In_2O_3 impurity in the starting material is indicated with a star.

crystalline $InVO_4$ was 99% phase pure with approximately 1% In_2O_3 impurity.

(b) Bulk samples of $InVO_3$ (98.5% purity) were synthesized by reduction of $InVO_4$ with carbon monoxide/carbon dioxide (1:1 volume ratio) in a flow tube at 450 °C for 12 h.

$$InVO_4 + CO \rightarrow InVO_3 + CO_2 \quad (2)$$

The low reaction temperature did not permit the formation of large crystallites as evidenced by the broadened diffraction peaks.

3.2. Room temperature powder X-ray diffraction

Product purities were determined with a Bragg–Brentano powder X-ray diffractometer (PANalytical X'Pert Pro) using Cu$K\alpha_{1,2}$ radiation equipped with a diffracted beam Ni-filter and an X'Celerator detector. Room temperature data sets were collected in the 2θ range 10–120° in 0.0167° steps. The powder X-ray diffraction data sets were analyzed by the Rietveld method using FullProf 2003 [17].

3.3. Powder neutron diffraction

Powder neutron diffraction data sets were collected on the medium-resolution 800 wire diffractometer C2 operated by the National Research Council Canada at Chalk River at room temperature and within a Janis closed cycle refrigerator. Diffractograms were measured at room temperature and at 3.1 K with neutron wavelengths $\lambda = 2.369(3)$ Å ($5° \leqslant 2\theta \leqslant 85°$) and $\lambda = 1.3315(6)$ Å ($35° \leqslant 2\theta \leqslant 115°$) and default detector wire spacing of 0.10° steps. Three-histogram Rietveld refinements using the room temperature diffraction data were carried out with the refinement package FullProf 2003 [17] for one X-ray and two neutron diffractograms with weights of 0.6, 0.2, and 0.2, respectively.

3.4. Thermogravimetric analysis (TGA)

TGA experiments were carried out with a Linseis L81 thermobalance. Polycrystalline $InVO_3$ was fully oxidized in Ar/O_2 with a linear heating rate of 10 °C/min from 25 to 1000 °C. All experiments were corrected for buoyancy and were conducted in alumina crucibles with Al_2O_3 powder (same mass as the sample) as the reference. Reduction experiments were carried out in CO/CO_2 flow (2:5). All reduction and oxidation products were identified by powder X-ray diffraction.

3.5. Magnetic measurements

Bulk d.c. magnetic susceptibility measurements were carried out with a Quantum Design MPMS SQUID magnetometer in the temperature range from 2 to 325 K and an applied magnetic field of 0.1 T. The samples were contained in gelatin capsules held in plastic straws.

4. Results and discussion

4.1. In situ powder X-ray diffraction

In situ powder X-ray diffraction data were collected during the reduction of polycrystalline $InVO_4$ (2% In_2O_3 impurity) in a 1:3 volume ratio of CO/CO_2. The temperature was ramped from 25 to 1000 °C using a 25 °C increment. Temperature-dependent diffraction data for a selected angular range are presented as a contour plot

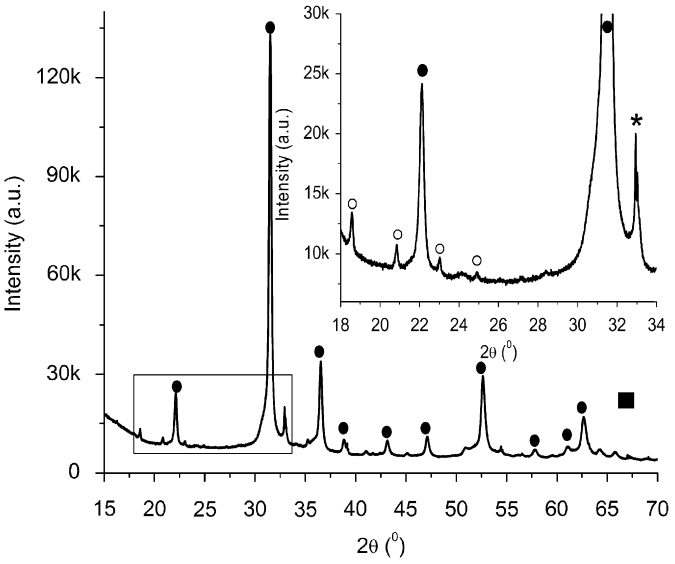

Fig. 2. Powder X-ray diffractogram of $InVO_4$ reduction in Ar/CO at 350 °C. Only the most intense $InVO_3$ peaks are labeled with solid circles. The inset emphasizes the presence of three phases: $InVO_4$ = open circles, $InVO_3$ = solid circles, In-metal = stars.

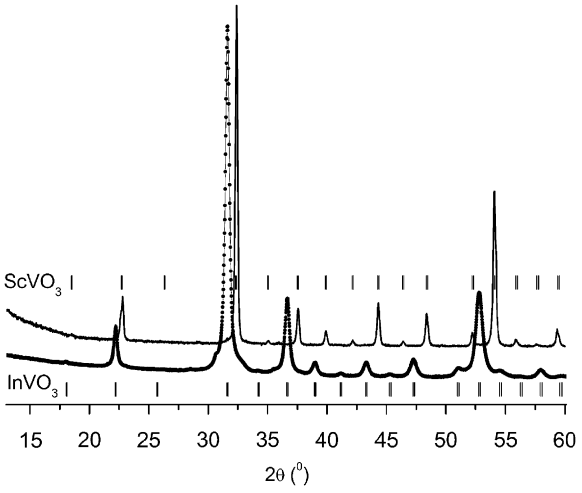

Fig. 3. Room temperature powder X-ray diffraction patterns of $InVO_3$ (bottom) and $ScVO_3$ (top). The expected Bragg positions are indicated below and above the respective patterns.

in Fig. 1. The $InVO_4$ peak intensities stay constant until approximately 400 °C. The peak intensities of $InVO_4$ decrease at 450 °C and the phase disappears entirely at 550 °C. Simultaneously, new broad peaks are observed at 450 °C which disappear again at 850 °C. At 600 °C peaks of the decomposition products In_2O_3 and V_2O_3 peaks are visible and remain until at least 1000 °C. The broad peaks visible for the temperature range 450–850 °C have been indexed on a cubic structure with unit cell parameter $a = 9.871(1)$ Å at 550 °C. The observed diffraction pattern at 550 °C resembles the bixbyite structure $ScVO_3$ (space group: *Ia−3*). A space group search for this new indium vanadium oxide phase revealed *Ia−3* (206) as the most likely candidate. This high-temperature in situ reduction of

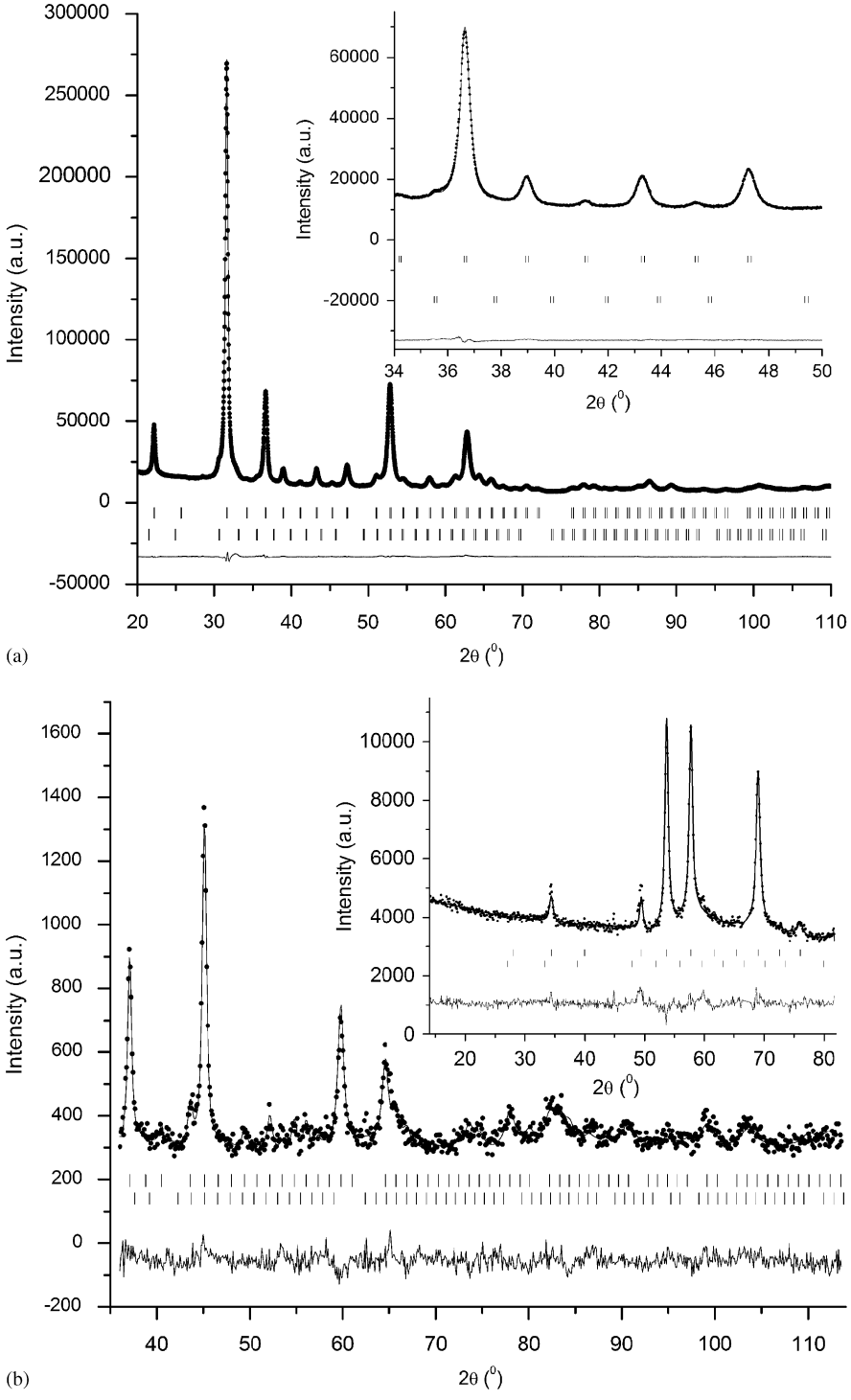

Fig. 4. Rietveld plots for powder Cu$K\alpha$ X-ray data (top) and neutron diffraction data (bottom, large $\lambda = 1.3302$ Å, inset $\lambda = 2.369$ Å). Experimental data points are shown as solid circles, the calculated patterns as solid lines, the differences as solid lines and the Bragg positions as vertical bars (upper set = $InVO_3$, lower set = In_2O_3).

$InVO_4$ suggests that a metastable bixbyite-type indium vanadium oxide structure can exist between 450 and 850 °C. We have identified this new phase as $InVO_3$. According to this in situ reduction phase pure $InVO_3$ can be obtained at 550 °C. Thermogravimetric reductions of $InVO_4$ to In_2O_3 and V_2O_3 in 1:3 volume ratio $CO:CO_2$ flow resulted in 6.88% mass loss confirming fully oxidized $InVO_{4.00(1)}$ starting material and only $V^{5+} \rightarrow V^{3+}$ reduction under these conditions.

It is noteworthy that $InVO_3$ can be observed as a transient intermediate in Ar/H_2 and in Ar/CO atmospheres. However no pure $InVO_3$ phase can be obtained, instead the starting material $InVO_4$ persisted while indium oxide was already reduced to indium metal. Fig. 2 shows a powder diffractogram of the reduction products. $InVO_3$ is the major phase (80% by mass) and impurity phases of unreacted $InVO_4$ and over-reduced In metal are present. Only the CO/CO_2 buffer gas provided a feasible atmosphere for the synthesis of pure $InVO_3$.

4.2. Bulk reduction of $InVO_4$ and crystal structure of $InVO_3$

A 3 g sample of polycrystalline $InVO_4$ was reduced for 12 h at 450 °C in CO/CO_2 (1:1 volume ratio) buffer gas. The homogeneous black product showed broadened powder X-ray diffraction peaks which were indexed on a cubic unit cell with $a = 9.80633(26)$ Å, a space group search suggested *Ia−3* (206) as the most likely candidate. This finding is in agreement with the intermediate phase identified at 550 °C during the in situ reduction of $InVO_4$. No additional superstructure peaks were identified. The diffraction pattern suggests that $InVO_3$ is isostructural with the $ScVO_3$ bixbyite structure (space group *Ia−3*, $a = 9.602$ Å) [9]. Fig. 3 shows the similar diffraction patterns for the above mentioned phases. Using the Rietveld refinement package FullProf 2003 the room temperature $InVO_3$ structure was refined against one X-ray and two neutron diffraction patterns using 0.6, 0.2 and 0.2 weighting factors, respectively. A total of 52 parameters have been refined including the background, scale factors, all zero points, neutron wavelengths, all peak shapes, atomic positions, isotropic temperature factors and site occupancies. The In/V ratio was refined independently for the 8*b* and the 24*d* sites using a constraint of fully occupied cation sites. For the In_2O_3 impurity phase only the scale factors and unit cell parameters were refined. The Rietveld plots are shown in Fig. 4. The best structural model of $InVO_3$ (see Table 1) indicates a one-to-one ratio of In^{3+} and V^{3+} ions on the 24*d* and 8*b* sites. Therefore, the In^{3+} and V^{3+} ions are randomly distributed with no site preference and the fractional occupancies result in a composition of $In_{0.99(1)}V_{1.01(1)}O_3$. The crystal structure is shown in Fig. 5 and selected bond distances and bond angles are listed in Table 2.

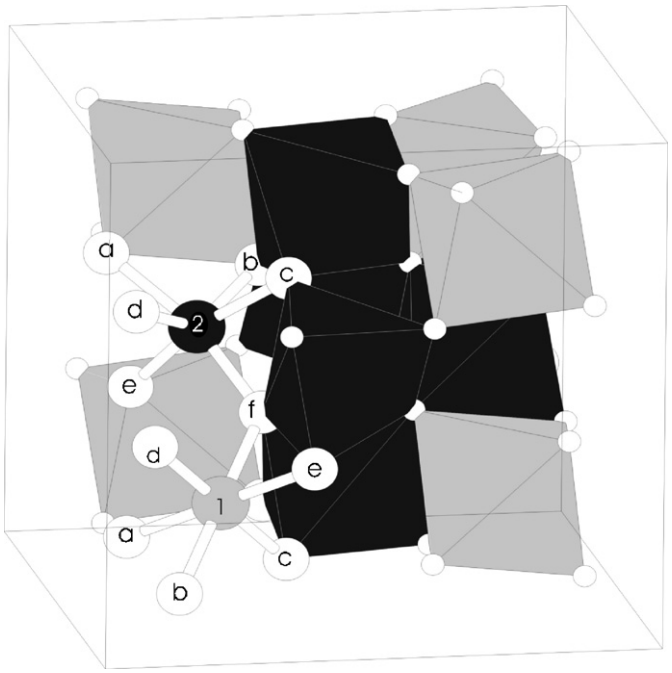

Fig. 5. $InVO_3$ bixbyite structure of (In/V)–O_6 octahedra. White spheres = oxygen, grey octahedra = In/V(1) 8*b* site, black octahedra = In/V(2) 24*d* site (for clarities sake only 1/4 of the 24*d* sites are shown).

Table 1
Room temperature structure of $InVO_3$ obtained from a combined Rietveld refinement against X-ray and neutron diffraction data

$InVO_3$	$a = 9.80636(31)$ Å		R_p(XRD)[a]:	2.11	R_{wp}(XRD):	2.87
	$V = 943.02(5)$ Å^3		R_p(NPD-1)[b]:	2.22	R_{wp}(NPD-1)[a]:	2.93
	Space group: *Ia−3* (206)		R_p(NPD-2)[c]:	2.30	R_{wp}(NPD-2)[a]:	3.05
	$Z = 16$		Global χ^2 :	10.8		
	Site	x	y	z	Frac. occ.	B_{iso} (Å^2)
In(1)	8*b*	1/4	1/4	1/4	0.49(1)	0.21(9)
V(1)	8*b*	1/4	1/4	1/4	0.51(1))	0.21(9)
In(2)	24*d*	0.96942(7)	0	1/4	0.49(1)	0.22(4)
V(2)	24*d*	0.96942(7)	0	1/4	0.51(1)	0.22(4)
O	48*e*	0.3931(4)	0.1515(4)	0.3868(4)	1.000	0.34(1)

The impurity phase In_2O_3 concentration was refined to 1.5(2) mass-percent.
[a]XRD = X-ray diffraction pattern with $\lambda = 1.54059$, 1.544426 Å (5978 data points, 2 phases, 210 reflections).
[b]NPD-1 = neutron diffraction pattern with $\lambda = 1.3315(6)$ Å (795 data points, 2 phases, 329 reflections).
[c]NPD-2 = neutron diffraction pattern with $\lambda = 2.369(3)$ Å (795 data points, 2 phases, 29 reflections).

Table 2
Selected bond distances and bond angles in $InVO_3$. The bonds and angles can be identified with the aid of Fig. 5

	Distances (Å)		Angles (deg)
In/V(1)–O	6 × 2.168(4)	O(a)–In/V(1)–O(b)	80.6(2)
		O(a)–In/V(1)–O(c)	80.6(2)
		O(b)–In/V(1)–O(c)	99.4(3)
		O(a)–In/V(1)–O(e)	180.0
		O(b)–In/V(1)–O(f)	180.0
In/V(2)–O(a,c)	2 × 2.147(4)	O(a)–In/V(2)–O(d)	75.9(2)
In/V(2)–O(b,d)	2 × 2.137(4)	O(a)–In/V(2)–O(e)	78.6(2)
In/V(2)–O(e,f)	2 × 2.005(4)	O(a)–In/V(2)–O(c)	112.9(3)
		O(f)–In/V(2)–O(d)	100.7(3)
		O(f)–In/V(2)–O(e)	90.6(3)
		O(f)–In/V(2)–O(b)	107.9(3)

Electron microprobe experiments confirmed a 1.00(2):1.00(2) indium to vanadium ratio in $InVO_3$. We also observed small amounts of In_2O_3 crystallites fused to the $InVO_3$ particles. Oxidative TGA in Ar/O_2 flow resulted in a mass gain of 7.38%. The expected gain for $InVO_3 + 1/2\ O_2 \rightarrow InVO_4$ is 7.48% for pure $InVO_3$. After correction for 1.5 mass-percent In_2O_3 impurity in the sample we confirm a stoichiometry of $InVO_{3.00(1)}$.

The low temperature preparation of $InVO_3$ only resulted in a poorly crystalline powder. Using the Scherrer equation (Eq. (3)) isotropic domain sizes of 225(50) Å have been estimated:

$$D = 0.9\lambda/B\cos(\theta), \tag{3}$$

where D is the domain size, λ the wavlength, B the integral breadth and θ the diffraction angle.

Attempts to anneal $InVO_3$ in argon failed due to product decomposition. In contrast to $InVO_3$ our $ScVO_3$ sample is highly crystalline with X-ray diffraction peak widths approaching the instrumental resolution. Since $InVO_3$ has been prepared at a fairly low temperature it cannot be assumed to be the thermodynamically stable phase, instead a kinetically favored product might have been obtained. Our in situ X-ray diffraction studies clearly indicate that the temperature range for a successful synthesis of $InVO_3$ is very narrow and that only gentle reduction of $InVO_4$ resulted in $InVO_3$ formation. The CO concentration is equally important; a 1:5 CO/CO_2 volume ratio did not reduce any appreciable amount of $InVO_4$, whereas pure CO results in the formation of indium metal. The direct reaction of In_2O_3 and V_2O_3 in an inert atmosphere did not yield $InVO_3$ but resulted in the recovery of the starting materials.

4.3. $InVO_3$ in relation to the AVO_3 series

The $LnVO_3$ series (Ln = La–Lu) forms a distorted perovskite structure ($GdFeO_3$ type), where Lu ($r(Lu^{3+}(VIII)) = 0.977$ Å) [18] is the smallest known perovskite forming A^{3+} cation for this series. For In^{3+} ($r(In^{3+}(VIII)) = 0.92$ Å) [18] no AVO_3 phase is known to date. The even smaller cation Sc^{3+} with $r(Sc^{3+}(VIII)) = 0.87$ Å [18] forms the disordered bixbyite structure, $ScVO_3$. The similar reduction potentials of $In^{3+} \rightarrow In^0$ and $V^{5+} \rightarrow V^{3+}$ limit the preparation of $InVO_3$ to very gentle reduction conditions and as indicated by the in situ reduction to a narrow temperature range. Thus, the existence of $InVO_3$ in the bixbyite structure is dependent upon the synthetic conditions rather than the thermodynamic stability of the phase. Consequently, no definite statement regarding the AVO_3 phase-stability as a function of the ionic radius can be derived from $InVO_3$. It is noteworthy that $InVO_3$ was predicted to crystallize in space $P6_3/mmc$.[16] To our knowledge this is the only albeit hypothetical mention of $InVO_3$ in the literature.

4.4. Magnetic properties of $InVO_3$

D.c. magnetic susceptibility measurements of $InVO_3$ were carried out between 5 and 325 K using a 0.1 T field (Fig. 6). The high-temperature d.c. magnetic susceptibility data between 245 and 325 K (Fig. 6 inset) were fitted with the Curie–Weiss law, $\chi = C/(T-\theta)$, where C = Curie constant, T = temperature and θ = Weiss temperature, a temperature-independent term was of no relevance. The following parameters were obtained: $C = 0.91(1)$ emu K/mol, $\mu_{eff} = 2.57(3)\,\mu_B$, $\theta = -134(5)$ K. The negative Weiss temperature indicates overall antiferromagnetic exchange interactions and the effective moment of 2.57 μ_B is less than the expected spin-only value of 2.82 μ_B for V^{3+}. However, the spin-only effective magnetic moment for V^{4+} of 1.73 μ_B is significantly lower than the experimental value for $InVO_3$. Note the curvature of the inverse susceptibility

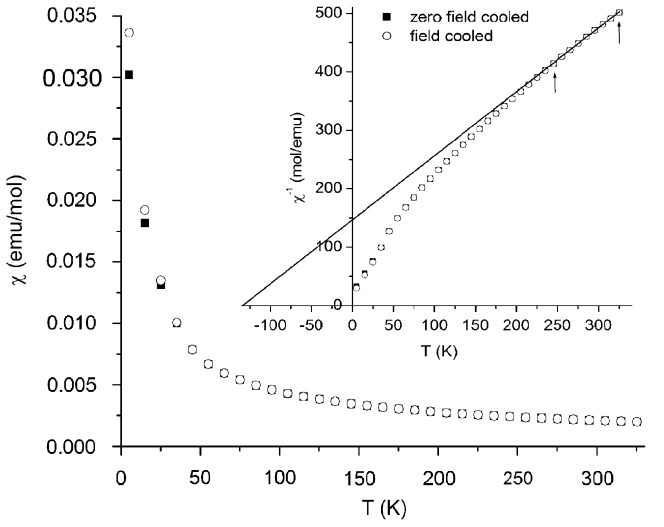

Fig. 6. D.c. magnetic susceptibility data collected using $H = 0.1$ T. Note the divergence of the ZFC (solid squares) and FC (open circles) data below 45 K. The inset shows the inverse magnetic susceptibility with the Curie–Weiss fit as a straight line (the fitting range is indicated by the arrows).

even at 325 K indicating that the true Curie–Weiss regime is above 325 K. The curvature reveals that the reported effective magnetic moment is a lower boundary. Thus, the experimental data strongly support the presence of V^{3+} in our sample. Fig. 6 suggests low temperature divergence of the zero field cooled (ZFC) and the field cooled (FC) data. Additional low-temperature d.c. magnetic susceptibility data from 2 to 60 K are shown in Fig. 7 showing ZFC–FC divergence below 55 K and a cusp at 3 K. The inflection point at 5 K is indicated with an arrow. The divergence and cusp may indicate a spin-glass type magnetic ground state. Low-temperature powder neutron diffraction data show no magnetic long-range ordering as evidenced by the absence of magnetic diffraction peaks at temperatures as low as 3.1 K. The 3.1 and 300 K neutron data are compared in Fig. 8. The presence of a spin-glass ground state is consistent with bond-disorder on a triangular cation sublattice due to the In^{3+}/V^{3+} disorder. A more in-depth investigation of the low-temperature magnetic ground state is in progress and will be reported elsewhere.

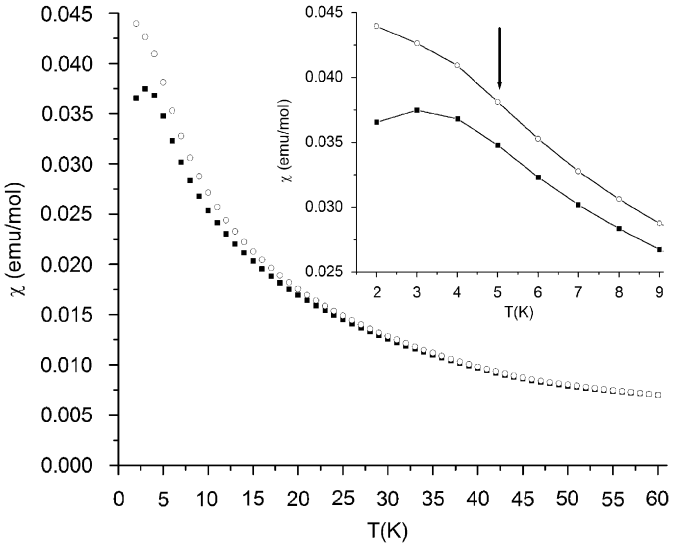

Fig. 7. Low-temperature d.c. magnetic susceptibility data collected using $H = 0.1$ T. Note the divergence of the ZFC (solid squares) and FC (open circles) data below 55 K. The inset emphasizes the cusp at 3 K and the inflection point at 5 K.

We would like to compare the d.c. magnetic susceptibility data of $InVO_3$ with $ScVO_3$. $ScVO_3$ reaches the Curie–Weiss regime at approximately 100 K and the Curie–Weiss fit reveals an effective magnetic moment $\mu_{eff} = 2.80(1)\,\mu_B$ for $ScVO_3$, this value agrees very well with the expected spin-only effective magnetic moment of $2.82\,\mu_B$ for V^{3+}. The Weiss temperature, $\theta = -115(2)$ K, indicates overall antiferromagnetic magnetic exchange interactions in $ScVO_3$. No features indicating magnetic ordering are visible between 5 and 325 K. In contrast to $InVO_3$ no significant ZFC–FC divergence is observed for $ScVO_3$.

5. Conclusions

We have reported for the first time the synthesis and structure determination of $InVO_3$. In situ powder X-ray diffraction revealed $InVO_3$ as a transient phase. Only very

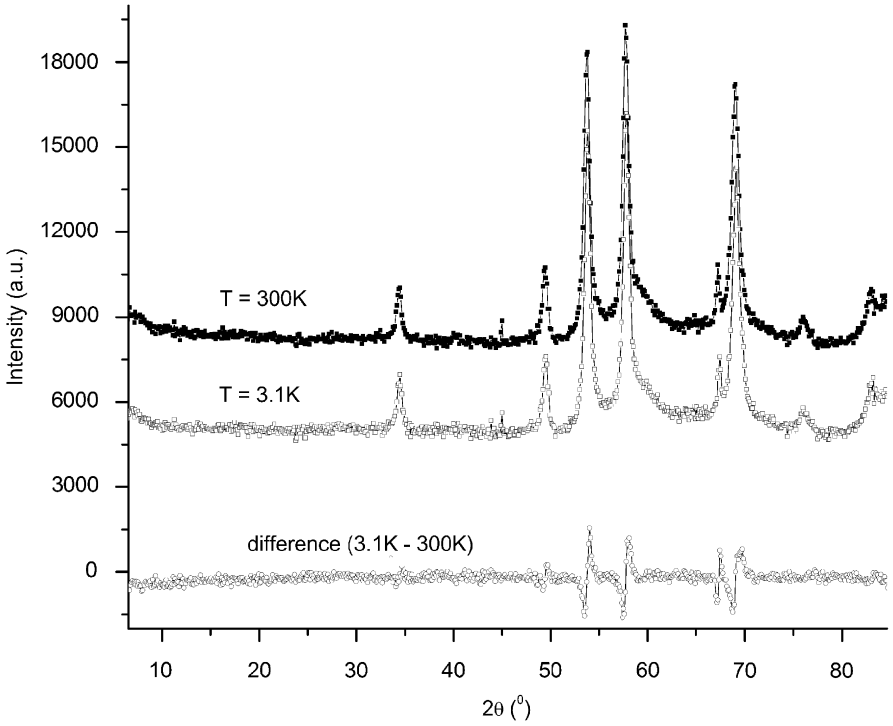

Fig. 8. Powder neutron diffraction patterns of $InVO_3$ at $T = 300$ and 3.1 K. No magnetic diffraction peaks are observed in the 3.1 K data set. The only differences relate to the unit cell contraction upon cooling.

gentle conditions permit the reduction of $InVO_4$ to pure $InVO_3$. The optimized conditions for the in situ synthesis are 550 °C using a 1:3 volume ratio of $CO:CO_2$ buffer gas. Higher temperatures resulted in In_2O_3 and V_2O_3 decomposition products, whereas harsher reduction conditions lead to the formation of indium metal. The bulk preparation of $InVO_3$ succeeded at 450 °C using 1:1 $CO:CO_2$ buffer gas. $InVO_3$ forms the bixbyite structure with In/V disorder with no preference either on the 8*b* or the 24*d* site. TGA experiments, microprobe analysis and the effective magnetic moment obtained from bulk magnetic susceptibility experiments confirm the composition $InVO_3$ and the V^{3+} oxidation state. No magnetic long-range order has been observed even at temperatures as low as 3.1 K. Low-temperature magnetization measurements suggest a spin-glass ground state for $InVO_3$.

Acknowledgments

The authors are grateful to Paul Dube (McMaster University), Roger Mitchell and Ruslan Liferovich (Lakehead University). MB gratefully acknowledges funding from NSERC and CFI. LMDC wishes to thank NRC technicians Raymond Sammon and Travis Dodd for assistance in setting-up the Janis closed cycle refrigerator system on C2.

References

[1] T. Mizokawa, D.I. Khomskii, G.A. Sawatzky, Phys. Rev. B 60 (1999) 7306–7313.
[2] J.-Q. Yan, J.-S. Zhou, J.B. Goodenough, Phys. Rev. B 72 (2005) 094412.
[3] A. Wold, R. Ward, J. Am. Chem. Soc. 76 (1954) 1029–1030.
[4] H.L. Yakel, Acta Crystallogr. 6 (1955) 394.
[5] P. Bordet, C. Chaillout, M. Marezio, Q. Huang, A. Santoro, S.-W. Cheong, H. Takagi, C.S. Oglesby, B. Batlogg, J. Solid State Chem. 106 (1993) 253–270.
[6] A. Munoz, J.A. Alonso, M.T. Casais, M.J. Martinez-Lope, J.L. Martinez, M.T. Fernandez-Diaz, Phys. Rev. B 68 (14) (2003) 144429/1–144429/11.
[7] A. Munoz, J.A. Alonso, M.T. Casais, M.J. Martinez-Lope., J.L. Martinez, M.T. Fernandez-Diaz, Chem. Mater. 16 (2004) 1544.
[8] A. Munoz, J.A. Alonso, M.T. Casais, M.J. Martinez-Lope, J.L. Martinez, M.T. Fernandez-Diaz, J. Mater. Chem. 13 (5) (2003) 1234.
[9] A.F. Reid, M.J. Sienko, Inorg. Chem. 6 (1967) 521.
[10] J.A. Alonso, M.T. Casais, M.J. Martinez-Lope, Dalton Trans. 9 (2004) 1294.
[11] S. Miyasaka, Y. Oimoto, M. Iwama, Y. Tokura, Phys. Rev. B. 68 (2003) 100406(R).
[12] J.B. Goodenough, Rep. Prog. Phys. 67 (2004) 1915–1993.
[13] H.C. Nguyen, J.B. Goodenough, Phys. Rev. B 52 (1) (1995) 324.
[14] H.C. Nguyen, J.B. Goodenough, J. Solid State Chem. 119 (1) (1995) 24.
[15] Y. Ren, T.T.M. Palstra, D.I. Khomskii, E. Pellegrin, A.A. Nugroho, A.A. Menovsky, G.A. Sawatzky, Nature 396 (6710) (1998) 441.
[16] D.M. Giaquinta, H.-C. zur Loye, Chem. Mater. 6 (1994) 365–372.
[17] J. Rodriguez-Carvajal, FullProf 2k, Vers. 3.20, 2005.
[18] R.D. Shannon, Acta Crystallogr. A 32 (1976) 751–767.